PAPER 53 – OPTIMIZING GEOPOLYMERIZATION PROCESS OF METABENTONITE-METAKAOLIN BASED GEOPOLYMER CONCRETE (BKGPC) USING RESPONSE SURFACE METHOD

A. Ahmed[1*], J. Abubakar[2], A. Lawan[3], A. Ocholi[4] and J. M. Kaura[5]

[1]Department of Civil Engineering, Federal University of Agriculture, Makurdi, Nigeria
[2]Department of Civil Engineering, Ahmadu Bello University, Zaria, Nigeria
[3]Department of Civil Engineering, Ahmadu Bello University, Zaria, Nigeria
[4]Department of Civil Engineering, Ahmadu Bello University, Zaria, Nigeria
Email: Amuinuahmed543@gmail.com

ABSTRACT
Carbon dioxide (CO_2) emissions from the production of Ordinary Portland Cement (OPC) contributed approximately 9% to greenhouse gases (GHGs) in the atmosphere which leads to global warming. Replacement of OPC in construction with supplementary cementitious materials (SCMs) is suggested by many researchers. Geopolymer concrete (GPC) strength characteristics for grades, mix proportions, and suitable precursors are major concerns in structural engineering. A mix design for a target compressive strength of 25 N/mm^2 with a Design of Experiment (DOE) using randomized block factorial design and laboratory investigations were conducted. Response Surface Method (RSM) analysis is employed for DOE and optimization of the geopolymerization process. Research findings in materials science and engineering led to the development of a mathematical model. The material was characterized using XRF and FTIR spectra, and the result of the XRF indicates that the chemical composition of the precursor conformed to BS EN 197:2011 for natural calcined pozzolans (Q). The FTIR result shows that polycondensation occurred at the end of the reaction and was accompanied by a water vaporization process. However, GPC exhibits a good compressive strength of 23.7 N/mm^2 with a NaOH molar concentration of 14 M and a Na_2Si_3O/NaOH ratio of 2.5 at a 28-day curing period.

Keywords: Geopolymer, Precursors, Alkaline, DOE, Optimization, Mathematical Model.

1. INTRODUCTION

Carbon dioxide (CO_2) emissions from the production of ordinary Portland cement (OPC) contributed approximately 9% to greenhouse gases (GHGs) in the atmosphere that lead to global warming (Mehta 2001; Lei et al., 2011). The replacement of OPC in construction with supplementary cementitious materials (SCMs) has been suggested by many researchers. Hafeez (2008); Karthikeyan et al. (2015) The geopolymerization process involves the activation of an alumino-silicate material or precursor from a geological source (meta bentonite, metakaolin) or an industrial by-product (fly ash, ground granulated blast furnace slag) with a strong alkali solution such as sodium silicates and sodium hydroxide, which is then mixed with aggregates to form a fresh geopolymer concrete (GPC) that is allowed to set, demoulded after 24 hours, and cured at 60 oC for another 24 hours (Xu and Van Deventer, 2000).

Researchers are suggesting partial or full replacement of ordinary Portland cement (OPC) in concrete construction with supplementary cementitious materials (SCMs) (Al-Bakri et al., 2011). Geopolymer is an emerging and innovative binder that can provide an environmentally friendly replacement for OPC (Bharat and Kamal, 2015). It has been estimated that geopolymer binder generates 85% less CO2 emissions and requires 60% less energy to manufacture than OPC (Duxson et al., 2007). Extensive research has been carried out on the development of geopolymer as a sustainable binder (Wallah and Rangan, 2021; Sumajouw and Rangan, 2006). Some recent studies have revealed that the positive effects of meta bentonite on the mechanical and microstructural properties of GPC are like those of conventional concrete with metabentonite or metakaolin. Mirza et al., 2009; Law et al., 2014). This study aimed at optimizing the geopolymer concrete strength parameters, and the following specific objectives were achieved: Establishing a mix design for a target compressive strength of 25 N/mm^2 and performing the design of experiment (DOE) using the Response Surface Method (RSM) conducting a laboratory experiment and using the exploratory data acquired from the lab to perform regression analysis and analysis of variance (ANOVA) to develop a mathematical model. Conducting microstructural characterization of the metabentonite/metakaolin-based geopolymer (BKGP) concrete products using Fourier transform infrared (FTIR) spectral Optimizing the response (compressive strength) properties of the BKGP concrete using RSM (Akbar et al., 2013)

2. THEORETICAL ANALYSIS

The polymerization process includes chemical reactions under highly alkaline conditions on Al-Si minerals, yielding polymeric Si-O-Al-O bonds as shown by equation (1), where M is the alkaline element, z is 1, 2, or 3, and n is the degree of polycondensation (Davidovits, 2008).

$$Mn\ [-(Si - O2)\ z - Al - O]\ n.H2O \quad (1)$$

Figure 1 shows the optimization of the geopolymerization process by reshuffling the precursor (metabentonite and metakaolin) and the alkali solution (sodium silicates and sodium hydroxide) to form the best constituent combination and the optimum strength characteristic of the hardened geopolymer concrete (Lima-Guerra et al., 2014).

2.1 Response Surface Method (RSM):

In RSM, the standard factorial in a randomized block design, choosing a model type depends on the nature of accessible information and levels for each factor. For the most part, for an experiment matrix that has been as of now built up, the historical data or user-defined model is applied for the development and investigation of a model **(**Myers and Montgomery, 2002).

The polynomial equation of the correlation between the response variables and independent variables can be expressed in a general form as shown in equation 2.

$$Y = \beta_0 + \Sigma_{i=1}^{k}\beta_i X_i + \Sigma_{i=1}^{k}\beta_{ii}X_{ii}^2 + \Sigma_{j=2}^{k}\Sigma_{i\le i\le j}^{j=1}\beta_{ij}X_iX_j + \varepsilon \quad (2)$$

Where Y is the response, xi and xj are the independent variables (i and j are the range from 1 to k), β_o is the constant coefficient, β_i, β_{ii},β_{ij} are the coefficient for the linear, quadratic and interaction effects, and ε represent the error. The coefficient of correlation (R^2), ranging from 0 to 1 was employed to predict the fitness of the developed model. A highly significant and accurate model is indicated by R^2 close to 1 (Montgomery, 2017).

2.2 Optimization

The desirability function approach is one of the most widely used methods in the industry for the optimization of the response process. It is based on the idea that the "quality" of a product or process that has multiple quality characteristics, with one of them outside of some "desired" limits, is completely unacceptable. The method finds operating conditions ***x*** that provide the "most desirable" response values.

For each response, Yi(x), a desirability function di(Yi) assigns numbers between 0 and 1 to the possible values of Yi, with di(Yi) = 0 representing a completely undesirable value of Yi and di(Yi) = 1 representing a completely desirable or ideal response value. The individual desirabilities are then combined using the geometric mean, which gives the overall desirability D:

$$D = (d_1(Y_1) \times d_2(Y_2) \times \ldots \times d_k(Y_k))^{1/k} \quad (3)$$

with **k** denoting the number of responses. Notice that if any response ***Yi*** is completely undesirable **(*di*(*Yi*) = 0)**, then the overall desirability is zero. In practice, fitted response values ***i*** are used in place of the ***Yi***.
If a response is of the "target is best" kind, then its desirability function is with the exponents ***s*** and ***t*** determining how important it is to hit the target value. For ***s* = *t* = 1**, the desirability function increases linearly towards ***Ti***; for ***s* < 1, *t* < 1**, the function is convex, and for ***s*> 1, *t* > 1**, the function is concave.

$$d_i(\hat{Y}_i) = \begin{cases} 0 & \text{if } \hat{Y}_i(\boldsymbol{x}) < L_i \\ \left(\frac{\hat{Y}_i(\boldsymbol{x})-L_i}{T_i-L_i}\right)^s & \text{if } L_i \le \hat{Y}_i(\boldsymbol{x}) \le T_i \\ \left(\frac{\hat{Y}_i(\boldsymbol{x})-U_i}{T_i-U_i}\right)^t & \text{if } T_i \le \hat{Y}_i(\boldsymbol{x}) \le U_i \\ 0 & \text{if } \hat{Y}_i(\boldsymbol{x}) > U_i \end{cases} \quad (4)$$

If a response is to be maximized instead, the individual desirability is defined as with

$$d_i(\hat{Y}_i) = \begin{cases} 0 & \text{if } \hat{Y}_i(\boldsymbol{x}) < L_i \\ \left(\frac{\hat{Y}_i(\boldsymbol{x})-L_i}{T_i-L_i}\right)^s & \text{if } L_i \le \hat{Y}_i(\boldsymbol{x}) \le T_i \\ 1.0 & \text{if } \hat{Y}_i(\boldsymbol{x}) > T_i \end{cases} \quad (5)$$

T*i* in this case interpreted as a large enough value for the response.
Finally, if we want to minimize a response, we could use **T*i*** denoting a small enough value for the response.

$$d_i(\hat{Y}_i) = \begin{cases} 1.0 & \text{if } \hat{Y}_i(x) < T_i \\ \left(\frac{\hat{Y}_i(x) - U_i}{T_i - U_i}\right)^s & \text{if } T_i \le \hat{Y}_i(x) \le U_i \\ 0 & \text{if } \hat{Y}_i(x) > U_i \end{cases} \quad (6)$$

3. MATERIALS AND METHODS

3.1 Raw Materials

The bentonite clay used in this study was sourced, beneficiated, and heated at 105 °C for 24 h to remove the water content. The dried bentonite was crushed and ground (3000 cycles) in a ball mill to increase its fineness as cement (range of 100 m), calcined at 650 °C for two hours to improve its chemical composition, and acquired the metabentonite. Kaolin clay was sourced and processed, ball milled and calcined at 700 °C for two hours to improve its chemical composition and obtain the metakaolin.

Table.1 Chemical composition of Metabentonite and Metakaolin.

Components	SiO2	Al2O3	Fe2O3	Na2O	CaO	MgO	K2O
Metabentonite	51.10	26.01	13.89	0.01	6.04	0.02	0.43
Metakaolin	52.43	42.22	1.90	0.29	0.17	0.17	0.61

Fine aggregate was sourced locally and coarse aggregate was sourced from the quarry site and supplied to the laboratory and tests were carried out following BS EN 933-1 and BS EN 12620. Alkali (Sodium Hydroxide and Sodium Silicates**)** was sourced from a chemical supplier. The NaOH was in pellet form while Na_2SiO_3 was in the form of gel.

3.2 Mix Design:

In the study, 22-factor designs were considered to test two factors, A (bentonite) and B (alkali doss), each measured in percentage. If A has (a = 5; 10, 20, 30, 40, and 50) levels and B has (b = 5; 50, 60, 70, 80, and 90) levels, each complete replicate of the experiment will contain (a × b = 5 × 5 = 25) runs (or treatment combinations) is most commonly used for two-level factorial designs where the main effect can be estimated as the average change of the response variable (y) when the factor is changed from its low to its high level (Caijun, 1996). The interactions between the variables (bentonite, kaolin, and the alkaline activator) and responses (compressive strength) were determined from diagnostic, ANOVA, and 2D and 3D contour plots. The volumetric percentage of bentonite precursor and alkaline activator were selected as the factors and were coded as A and B, respectively, as shown in Table 1.

Table 1: Factors and Factor Levels Adopted

Factor	Name	Units	Type	Sub Type	Min.	Max.	Coded Low	Coded High	Mean	Std. Dev.
A	Metabentonite	%	Numeric	Discrete	10.00	50.00	-1	+1	30.00	14.19
B	Alkali Dosage	%	Numeric	Discrete	50.00	90.00	-1	+1	70.00	14.19

Twenty-five proportions of geopolymer concrete were used in this experiment for cube samples. The substitution of metakaolin by metabentonite was done in geopolymer concrete mixes at varying metabentonite proportions of (10 %, 20 %, 30%, 40% and 50 %) with five different volumetric percentages of alkaline activators of (50 %, 60 %, 70, 80, and 90 %) by mean DOE using randomized block factorial design in Design Expert 13.

3.3 Mixing Procedure for Geopolymer Concrete

The mixing method for geopolymer concrete was performed by adopting the traditional techniques used in the production of normal concrete. Firstly, all materials (bentonite, kaolin, fine aggregate, and coarse aggregate) were mixed in a dry condition in the concrete mixer for approximately three minutes (Pavithra et al., 2016). The alkaline solution was mixed for approximately two minutes. After that, the liquid activator component was added to the dry materials and mixed for four minutes in the concrete mixer (Rangan, 2011).

3.4 Preparation of Alkaline Solution for Geopolymer

The alkali activator materials (AAMs) are constituted of sodium silicate and sodium hydroxide and were mixed, stirred, and shaken for two minutes before use. The ratio of sodium silicates to sodium hydroxide (Na_2SiO_3/NaOH) used in this experiment was 2.5. Sodium hydroxide in pellet form has a high purity of more than 98% and could be dissolved in potable water 24 hours before use. The solutions had a suitable molecular concentration of 14 M. Twenty-four hours after preparation, NaOH solutions were added to the Na_2SiO_3 solutions for a 2.5 mix ratio.

3.5 Test Methods

The data to be followed in the developed models using RSM for optimization were evaluated in the laboratory analysis. To evaluate the mutual correlation with the variables, compressive strength at 28 days as a property of geopolymer concrete was taken as the response of interest. The geopolymer concrete specimens were cast, demolded after 24 hours, and oven dried at 600 °C for another 24 hours. The curing periods were 28 days for all the samples. The dry specimens were tested according to Provis and Van Deventer (2009) standards.

4. RESULTS AND DISCUSSION

4.1 Bonding Nature by FT-IR Spectra Analysis

Figure 2 shows the IR spectra of a metabentonite/metakaolin-based geopolymer (BKGP) concrete product with a 14 M molar concentration of NaOH and a Na_2SiO_3/NaOH ratio of 2.5. The IR spectral for BKGP concrete has the following bands: The vibrational frequency around 1006.4 cm-1 corresponding to the precursor material is shifted to 872 cm-1; this is due to the penetration of Al4+ atoms into the initial Si-O-Si-skeletal structures. The condensation of Si-O tetrahedra in geopolymer paste was confirmed. Symmetric stretching vibrations of -Si-O-Si- and -Al-O-Si- can also be identified near 730 cm1 and bending vibrations of -Si-O-Si- and -O-Si-O- in the 689 cm1 regions. The bending vibration of 1442.5 cm^{-1} corresponding to the CO_3^{2-} carbonate groups, 1651.2 cm-1 for H_2O crystallized, and 1792.8, 1919.6, 1979.2, 2102.2, and 2325.9 cm-1 vibrational plane Si-O

The absorption bands for BKGP concrete at (3194.3, 3254, 3339.7, 3432.9, 3466.4, 3567.1, 3645.3, 3675.2, and 3757.2 cm1) were observed due to the occurrence of stretching vibration of the -OH groups or bonded water. This result indicates that crystalline structures have been dissociated and changed due to the alkali activation process. The resulting silica-aluminium oxide species then reacted and formed oligomeric precursors. Furthermore, polycondensation occurs at the end of the reaction and is accompanied by the water vaporization process and this conforms to Brough and Atkinson (2002), Yang et al. (2020), and Fernandez-Jimenez and Palomo (2005).

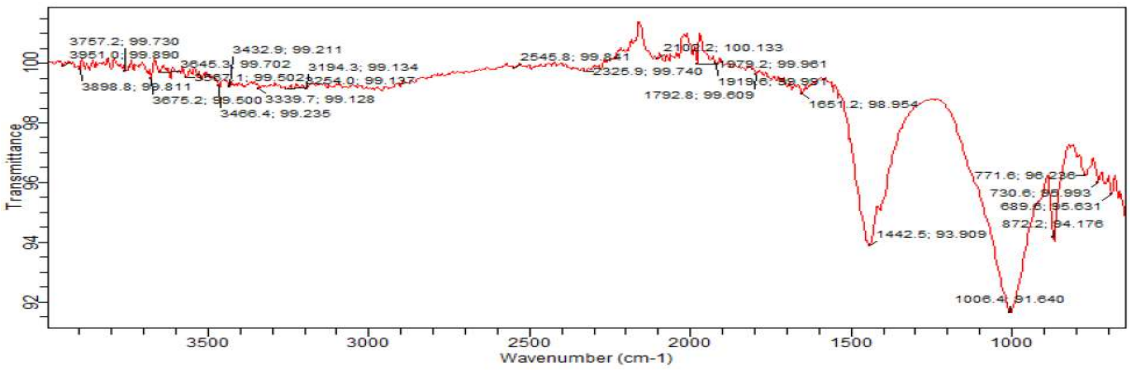

Figure 2: Shows the IR spectral for (BKGP) concrete product.

4.2 Response Surface Optimization:

The experimental data were made per the suggested DOE input from RSM. The resultant compressive strength of different mixes has been determined as a step for further analysis. The regression coefficient obtained for the experimental design, along with their corresponding p-values, are tabulated and shown in Table 2.

The p-value is 0.05, showing the high significance of all the input parameters, and it was considered for the construction of the RS model. The resulting regression model obtained an R-squared value of 84.54%, and the coefficients of determination (R-squared) are very near 100%, indicating the best fit of the data to the model assumed.

Table 2: Regression co-efficient for the RSM model.

Std. Dev.	0.84	**R^2**	0.85
Mean	20.28	**Adjusted R^2**	0.83
C.V. %	4.16	**Predicted R^2**	0.82
p-value	<0.01	**Adeq Precision**	37.87

The final model for 28 d compressive strength **CP8M2.0** of all mixes comprising all the terms is presented in Equation (7).

$$\textbf{(CP8M2.0)}^{1} = 22.84 + 0.6\,A + 1.02\,B + 2.56\,AB - 5.82\,A^2 - 2.33\,B^2 - 1.58\,A2B - 1.63\,AB^2 - 1.10\,A^2B^2 - 2.11\,A^3B - 2.84\,AB^3 + 4.19\,A^4 \quad (7)$$

The properties of formulated model for 28 d compressive strength **CP8M2.0** of the mix were presented in Table 2. The adequacy of the formulated models was validated by their degree of correlation (R^2). A high degree of correlation (R^2) was observed for the model based on their values being close to unity ($R^2 > 0.84$).

4.2 Analysis of Variance:

Diagnostic plots are vital to see if assumptions are met. Figure 3 shows the residual plot and regression diagram exhibiting the fits and the experimental observation for the attribute, compressive strength. As observed, there are no significant deviations from the normal probability line, and it can be fairly concluded that the assumptions of normality are satisfied.

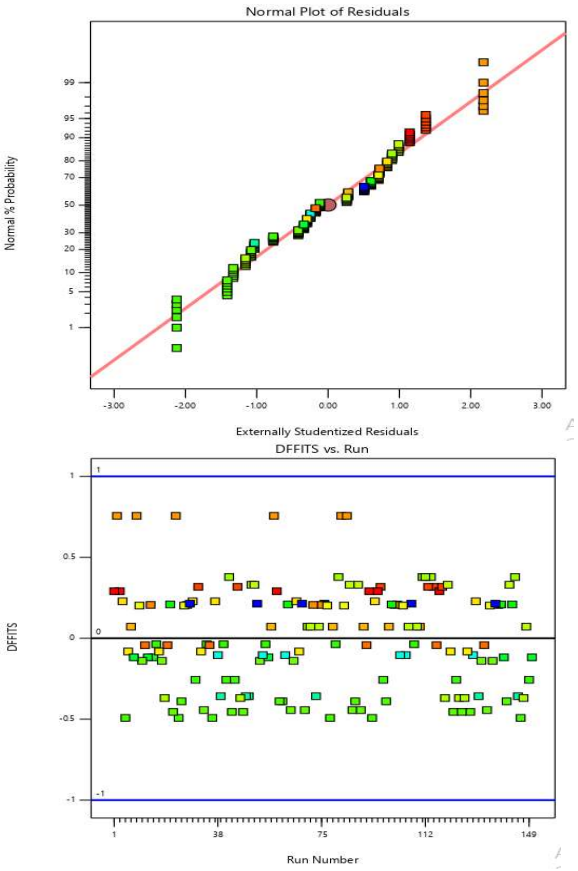

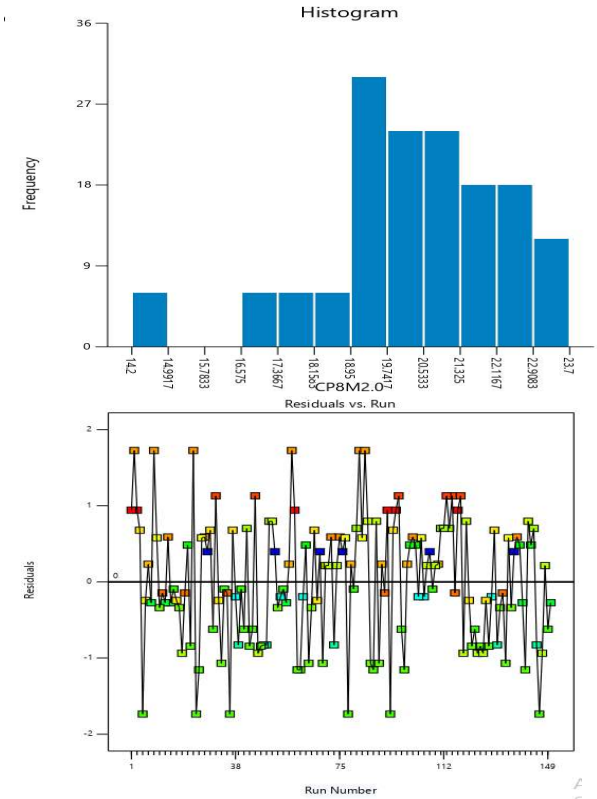

Figure 3. Residual plots for 28 d compressive strength **CP8M2.0** (Mpa) of BKGP concrete

The degree of influence on compressive strength and interactions among factors are described in Figure 4. The shape of the 3D response surface and contour can reflect the degree of interaction. Figure 4 is steep and elliptical as it represents significant interactions between the factors and this is similar to the result obtained by Petrus et al. (2016) and Danek et al. (2015).

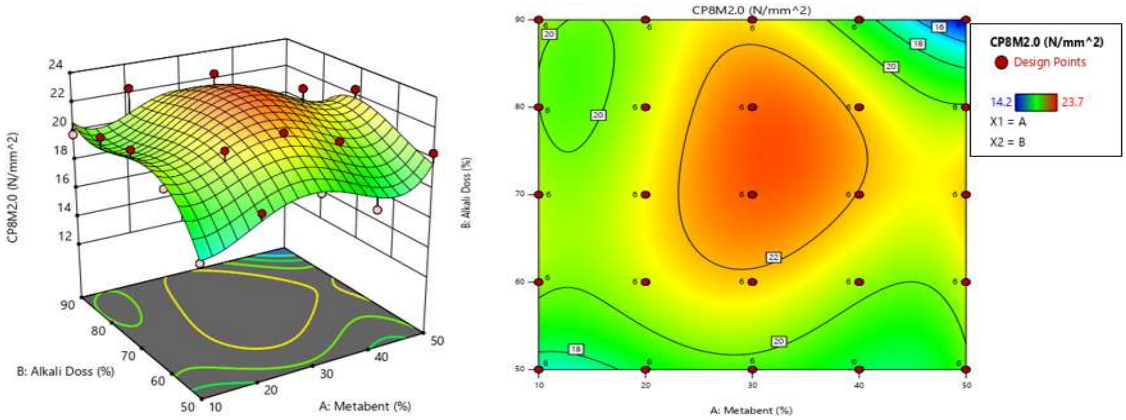

Figure 4. 3D-RS and contour plots showing the relation between Metabentonite, Alkaline dosage and strength

Figure 5 shows that the optimization of the 28-d compressive strength CP8M2.0 (Mpa) of BKGP concrete was at an optimum value of 23N/mm^2 and 96.8% desirability, and the percentage of metabentonite and alkaline dosage was 31.7% and 74.8%, respectively. This complies with Huang (2020).

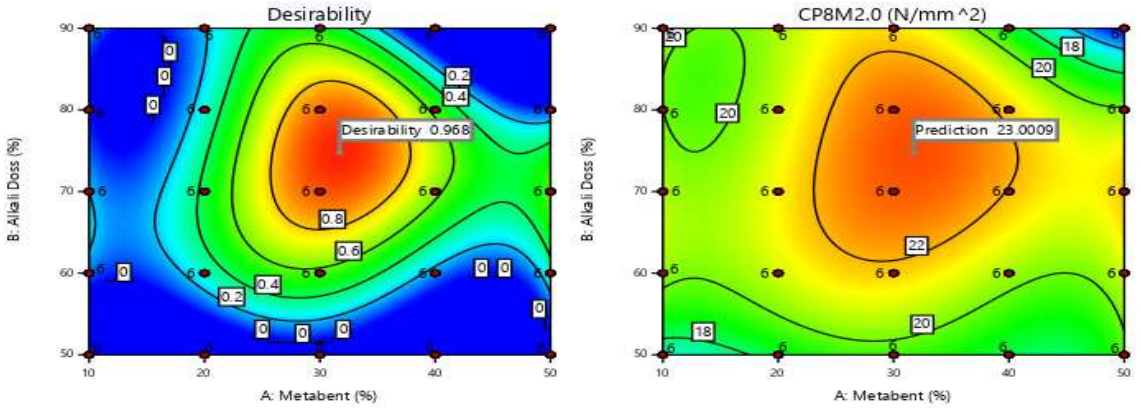

Figure 5: 2D-RS of Desirability and Optimum value of CP8M2.0 relations with factors (Metabentonite and Alkaline dosage)

5. CONCLUSIONS

Based on the experiments and analyses performed, the following conclusions were drawn:

i. The incorporation of metabentonite in metakaolin-based geopolymer concrete (GPC) is a step to further improve environmental sustainability. The formation of the matrix was due to the geopolymerization reaction that occurred.

ii. The mechanical properties of BKGP concrete are directly proportional to the bentonite substitution. About 31% of metabentonite showed maximum compressive strength among all BKGP concrete mixes due to the pozzolanic nature of the metabentonite/metakaolin-blend and alkali activation.

iii. The optimum preparation parameters are a metabentonite-metakaolin ratio of 31.7%, an alkali dosage of 74.8%, and a sodium silicate modulus of 2.5%. The maximum strength is predicted to be 23 MPa based on the optimum preparation parameters.

iv. The metabentonite/metakaolin-based geopolymer concrete with 23.6 MPa was prepared, which exhibited a relative error of 2.54%.

v. Metabentonite and metakaolin blended geopolymer BKGP concrete can be utilized as supplementary precursor material in geopolymer concrete upon thorough investigation (physical and chemical properties).

vi. BKGP concrete can be recommended as a sustainable concrete technology to reduce GHGs and global warming and can be utilized as a structural concrete material for residential construction and industrial infrastructure.

ACKNOWLEDGEMENT

The authors would like to thank every person or department that helped throughout the research. The supervisory team and the Civil Engineering Department, Ahmadu Bello University, Zaria Their careful reviews and constructive suggestions are gratefully acknowledged.

REFERENCE

Akbar. J, Bashir Alam, Muhammad Ashraf, Salman Afzal, Asfandyar Ahmad, and Khan Shahzada. (2013). "Evaluating the Effect of Bentonite on Strength and Durability of High PerformanceConcrete," *International Journal of Advanced Structures and Geotechnical Engineering*, vol. 02, no. 01, pp. 1–5.

Al-Bakri, M.M.; Mohammed, H.; Kamarudin, H.; Niza, I.K.; Zarina, Y. (2011). Review on fly Ash-based geopolymer concrete without Portland Cement. *J. Eng. Technol*. Res. 3, pp. 1–4.

Bharat B and Kamal K (2015) '' Geopolymer concrete-A Review'' *SSRG International Journal of Civil Engineering (SSRG-IJCE),* ISSN: 2348 – 8352, pp. 96-99.

Brough, A. R. and Atkinson, A. (2002). "Sodium silicate-based, alkali-activated slag mortars: Part I. Strength, hydration and microstructure. "*Cement and Concrete Research* 32(6), pp. 865-879.

Caijun, Shi. (1996). Strength, pore structure and permeability of alkali-activated slag mortars, *Cem. Concr. Res*. pp.

1789.

Danek, T.; Thomas, J.; Jelinek, J.(2015). Study of Interaction between Fly Ash-cement and Bentonite Matrices. *MATEC Web Conf*. 26, pp. 1003.

Davidovits, J., (2008). Geopolymer, Chemistry and Applications, *Institute of Geopolymer, 3rd(Ed),* France, Saint-Quentin. pp. 585.

Duxson, P.; Provis, J.L.; Lukey, G.C.; Van Deventer, J.S. (2007). The role of inorganic polymer technology in the development of green concrete. *Cem. Concr. Res.* 37, pp. 1590–1597.

Fernandez- Jimenez A. and J. Palomo, (2005*).* Composition and microstructure of alkali-activated fly ash mortar: effect of the activator, *Cem. Concr. Res*. pp. 1984.

Hafeez S.M., (2008). Preparation and Characterization of the Non-Portland Cement.*M.SC. Thesis, Zagazig Univ: Faculty of Science, Egypt*.

Huang, Y. (2020). Influence of Calcium Bentonite Addition on the Compressive Strength, Efflorescence Extent and Drying Shrinkage of Fly-Ash Based Geopolymer Mortar. *Trans. Indian Ceram. Soc*. 79, pp. 77–82.

Karthikeyan, M.; Ramachandran, P.R.; Nandhini, A.; Vinodha, R.(2015). Application of partial substitute of cement by bentonite in concrete. *Int. J. ChemTech Res*. 8, pp. 384–388.

Law, D., Adam, A., Molyneaux, T., Patnaikuni, I. and Wardhono, A. (2014*).* "Long-term durability properties of a class F fly ash geopolymer concrete." *Materials and Structures:* pp. 1-11.

Lei, Y. Zhang, Q. Nielsen, C., He, K.(2011). An inventory of primary air pollutants and CO2 emissions from cement production in China, 1990–2020. *Atmos. Environ*. 45, pp. 147–154.

Lima-Guerra, D.J.;Mello, I.; Resende, R.; Silva, R. (2014). Use of Bentonite and Organo bentonite as Alternatives of Partial Substitution of Cement in Concrete Manufacturing. *Int. J. Concr. Struct. Mater*. 8, pp. 15–26.

Mehta, P. K. (2001). *"*Reducing the Environmental Impact of Concrete" *ACI Concrete International* 23(10): pp. 61-66

Mirza, J.; Riaz, M.; Naseer, A.; Rehman, F.; Khan, A.; Ali, Q. (2009). Pakistani bentonite in mortars and concrete as low-cost construction material. *Appl. Clay Sci.* 45, pp. 220–226.

Montgomery DC (2017) *Design and Analysis of Experiments*, John Wiley and Sons.

Myers, R.H. and Montgomery, D.C. (2002) Response Surface Methodology: Product and Process Optimization Using Designed Experiments. 2nd Edition, John Wiley and Sons, New York

Pavithra, P.E.; Reddy, M.S.; Dinakar, P.; Rao, B.H.; Satpathy, B.; Mohanty, A. A (2016). Mix design procedure for geopolymer concrete with fly ash. *J. Clean. Prod*. 133, pp. 117–125.

Petrus, H.T.B.M.; Hulu, J.; Dalton, G.S.; Malinda, E.; Prakosa, R.A. (2016). Effect of Bentonite Addition on Geopolymer Concrete from Geothermal Silica. *Mater. Sci. Forum,* 841, pp. 7–15.

Provis, J. L. and Van Deventer, J. S. J. (2009). Geopolymer: structure, processing, properties and industrial applications. *J. L. Provis and J. S. J. Van Deventer. Boca Raton, Fla*: CRC

Rangan. B.V. (2011) ''Fly ash based geopolymer concrete'', *proceeding of International Workshop on Geopolymer cement and Concrete, Mumbai, India, December*, pp. 68-106

Sumajouw, M.; Rangan, B.V. (2006). Low-Calcium Fly Ash-Based Geopolymer Concrete: Reinforced Beams and Columns; *Curtin University of Technology: Perth, Australia*,

Wallah, S.; Rangan, B.V. (2021). Low-Calcium Fly Ash-Based Geopolymer Concrete: Long-Term Properties; *Curtin University of Technology: Perth, Australia, 2006.*Materials 14, 7790, pp. 21 of 23

Xu, H. and Van Deventer, J. S. J. (2000). "The geopolymerisation of alumino-silicate minerals." *International Journal of Mineral Processing* 59(3): pp. 247-266.

Yang, Y.; Jiang, J.; Hou, L.; Lu, Z.; Li, J.; Wang, J. (2020). Pore structure and properties of porous geopolymer based on pre-swelled bentonite. *Constr. Build. Mater*. 254, pp. 119-226.